Scripta Materialia 115 (2016) 91–95

Contents lists available at ScienceDirect

Scripta Materialia

journal homepage: www.elsevier.com/locate/scriptamat

Regular Article

New insights into the corrosion of magnesium alloys — The role of aluminum

M. Esmaily [a,*], D.B. Blücher [b], J.E. Svensson [a], M. Halvarsson [c], L.G. Johansson [a]

[a] Department of Chemistry and Chemical Engineering, Chalmers University of Technology, SE-412 96 Gothenburg, Sweden
[b] SINTEF Materials and Chemistry, N-7465 Trondheim, Norway
[c] Department of Applied Physics, Chalmers University of Technology, SE-412 96 Gothenburg, Sweden

ARTICLE INFO

Article history:
Received 24 November 2015
Received in revised form 3 January 2016
Accepted 4 January 2016
Available online 24 January 2016

Keywords:
Magnesium alloys
Atmospheric corrosion
Surface film
Aluminum

ABSTRACT

The atmospheric corrosion of several Mg–Al alloys was investigated at −4, 4 and 22 °C. The rate of corrosion increased with increasing temperature and decreasing Al content. Also, the effect of temperature became stronger with increasing Al content. The cast microstructure was found to influence both the average corrosion rate and the temperature dependence of corrosion. The influence of Al on corrosion and on the temperature dependence of corrosion is discussed in terms of the Al enriched layer in the bottom of the surface film and the breakdown of the same layer by chloride ions.

Environmental degradation is a limiting factor for magnesium–aluminum (Mg–Al) alloys in outdoor applications. Thus, Mg corrosion and Mg alloy corrosion have been the subject of numerous studies during the last two decades [1–13]. There is an ongoing discussion regarding the mechanism of Mg corrosion [1–3]. The effects of environmental variables on the corrosion of Mg–Al systems have been studied [4,5]. Also, there are extensive studies on the role of microstructure in the corrosion of Mg alloys [6–10]. For instance, it has been shown that Mg alloys fabricated by rheocasting (RC) exhibit significantly better corrosion resistance than their counterparts produced by high pressure die casting (HPDC) [11,12]. Despite these research efforts, the influence of temperature on atmospheric corrosion of Mg–Al alloys is largely unexplored. A recent study has shown that while the corrosion of alloy AM50 exhibits a strong temperature-dependence, 99.97% Mg does not [13]. The atmospheric corrosion of Mg–Al alloys at low temperatures is of interest especially in automotive applications. This is because in many regions cars are exposed to severe corrosive conditions during winter, due to the use of de-icing salt. Other important unresolved issues in the atmospheric corrosion of Mg–Al alloys include how exactly Al and chloride (Cl^-) ions influence the protective character of the quasi-passive surface films.

This study addresses the composition of the surface films formed on AZ91D produced by the RC method exposed at 22, 4 and −4 °C. The aim was to shed more light on the role of Al in the corrosion of Mg alloys and on the mechanisms by which the surface film is disrupted by Cl^-. The analyses were performed using high-resolution Auger electron spectroscopy (AES) in a site-specific manner on α-Mg grains and on the inter-dendritic regions. Details of the exposures are described elsewhere [13]. The corrosion products were analyzed by X-ray diffraction (XRD) and X-ray photoelectron spectroscopy (XPS). We investigated pure Mg (taken from an ingot) as well as several Mg–Al alloys. It should be mentioned that the Fe (~18 ppm) and Ni (~3 ppm) contents of the pure Mg were well below the respective tolerance limits as reported by [14–16]. This was also true for the alloys tested.

The gravimetric results for alloy AZ91D in the RC and HPDC states in Fig. 1a show that the corrosion rate depended strongly on temperature. Also, RC AZ91D exhibited better corrosion resistance than HPDC AZ91D at all three temperatures. The authors have previously discussed the reasons behind the superior corrosion resistance of RC materials [11,12]. The somewhat higher Al content in the α-Mg grains of the RC materials was suggested to be one of the explanations. Interestingly, the results showed that the beneficial effect of microstructure on the corrosion of Mg–Al alloys also depended on temperature (Fig. 1a). Thus, while the average corrosion rate of the HPDC material was ~1.5 times that of the RC alloy at 22 °C, the corresponding factor at −4 °C was ~7.5. To explore how the solidification microstructure affects alloy corrosion at different temperatures, the microstructure and composition of the corrosion products and surface films was subjected to detailed analysis.

The corrosion products formed at 4 and 22 °C were similar (Fig. 1b). $Mg_5(CO_3)_4(OH)_2 \times 4H_2O$ (hydromagnesite) was the dominant corrosion product. Traces of $Mg_5(CO_3)_4(OH)_2 \times 5H_2O$ was also detected. In contrast, at −4 °C, hydroxy carbonates were absent. Instead, two diffraction peaks were observed that belonged to corrosion products but that could not be attributed to any known compound [13]. The peaks appeared irrespective of the presence of NaCl, CO_2 and Al content, implying that it is a compound of magnesium and oxygen and/or

* Corresponding author.
E-mail address: mohsen.esmaily@chalmers.se (M. Esmaily).

http://dx.doi.org/10.1016/j.scriptamat.2016.01.008

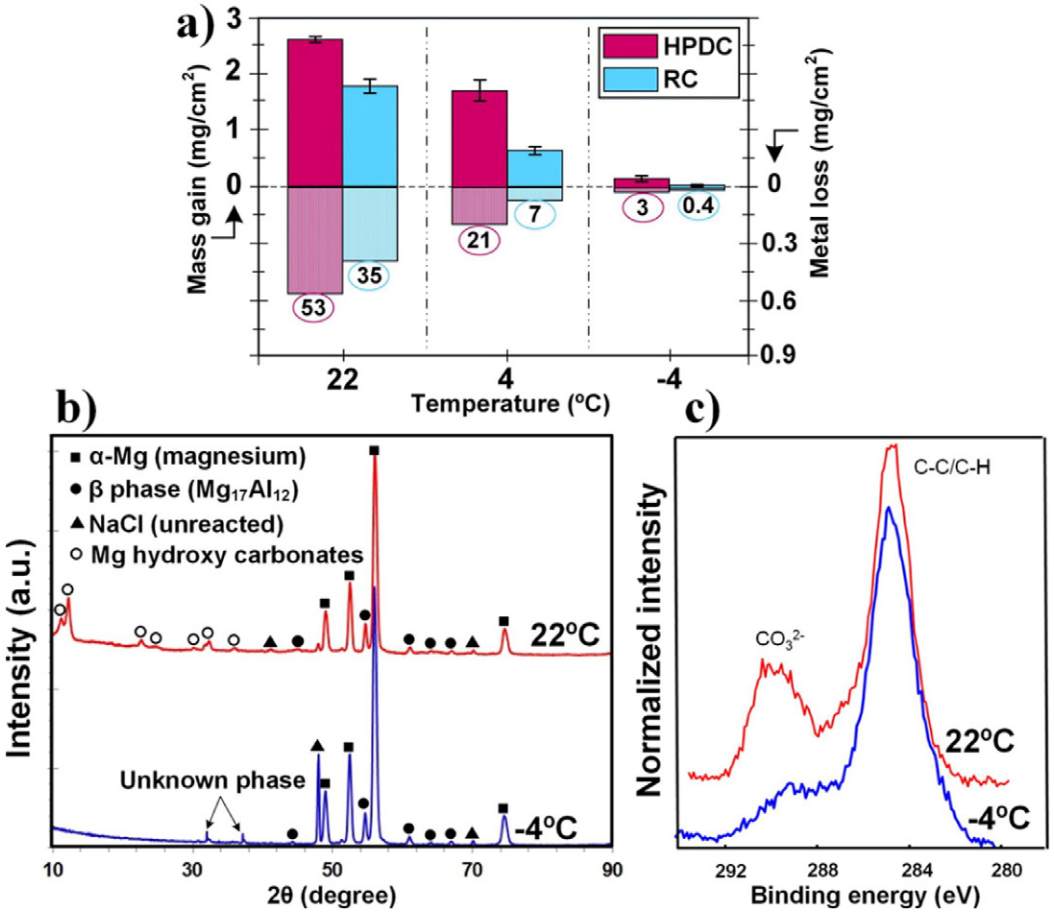

Fig. 1. (a) Mass gain and metal loss of RC and HPDC AZ91D (after 672 h). Corrosion rates (μm/year) are given beneath the metal loss bars. (b) XRD patterns recorded after the exposures in Fig. 1a at −4 and 22 °C. (c) XPS spectra from alloy AZ91D exposed in the absence of NaCl at −4 and 22 °C after 672 h.

hydrogen, possibly a low-temperature form of Mg hydroxide. The XPS spectra in Fig. 1c show the C1s peak after 672 h in the absence of NaCl at −4 and 22 °C. The peak at ~290 eV corresponds to carbon in CO_3^{2-}. In line with the XRD results, at 22 °C, a strong CO_3^{2-} peak was detected, while at −4 °C, a much weaker CO_3^{2-} peak was present.

Fig. 2 shows corrosion rates of the alloys. The rate of corrosion decreased strongly with increasing Al content. Pure Mg showed no clear correlation between corrosion rate and temperature. In contrast, alloys exhibited a positive correlation between temperature and corrosion rate. Importantly, the effect of temperature on corrosion was proportional to Al content. In the case of AM20, lowering the exposure temperature from 22 to −4 °C only resulted in a 15% decrease in corrosion rate,

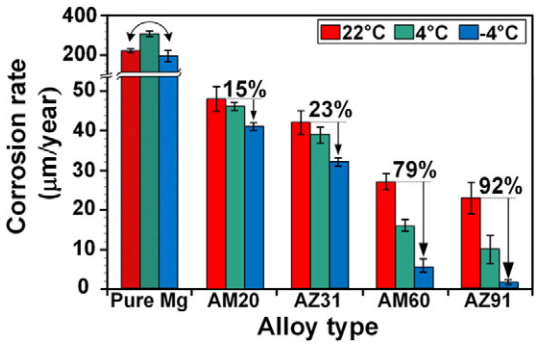

Fig. 2. Corrosion rate of 99.97% Mg and four HPDC Mg–Al alloys (RH: 95%, CO_2: 400 ppm, NaCl: 70 μg/cm², time: 504 h). The decrease in the corrosion rate from 22 to −4 °C is given as a percentage.

while the same decrease in temperature resulted in a 92% decrease in the corrosion of AZ91D.

It is interesting to note that pure Mg corroded faster than the alloys. This is not consistent with some results presented in the literature. Thus, Liu et al. [16] reports that during immersion in 3% NaCl (*aq*) solution, the corrosion of Mg alloys was greater than that of high purity Mg. This implies that the relative rate of corrosion of Mg and Mg–Al alloys during exposure to the atmosphere is different from that observed in immersion test conditions. The observed discrepancy is attributed to differences in the corrosion mechanism during atmospheric exposure in the presence of NaCl as compared to NaCl (*aq*) immersion testing. This topic is beyond the scope of this letter and will be addressed in a future study.

AES compositional depth profiling (Fig. 3) was carried out to investigate the chemistry of the surface films formed on RC AZ91D exposed in a NaCl-free environment. The analyses were performed on the middle of α-Mg grains with ~35 μm diameter containing 3.5 ± 0.1 wt.% Al. In all cases, we reached to the alloy substrate, which exhibited a weak O signal and strong Mg and Al signals (Fig. 3). The surface film formed at −4 °C was much thinner (~22 nm, Fig. 3a) than at 22 °C (~130 nm, Fig. 3c). Irrespective of temperature, the top 5 nm of the surface films had a high atomic percentage of C due to surface contamination. The top part of the film was made of hydromagnesite (in line with the XPS spectra in Fig. 1c). Deeper into the film the O/Mg ratio decreased to about 2, indicating the presence of $Mg(OH)_2$. The lack of evidence for MgO in the film in Fig. 3 does not rule out the presence of a thin MgO layer at the film/metal interface, as reported by [7,17,18], see also Fig. 4. Small amounts of Al^{3+} were indeed detected in the film. In contrast to the films formed at 4 and 22 °C, the film formed at −4 °C did

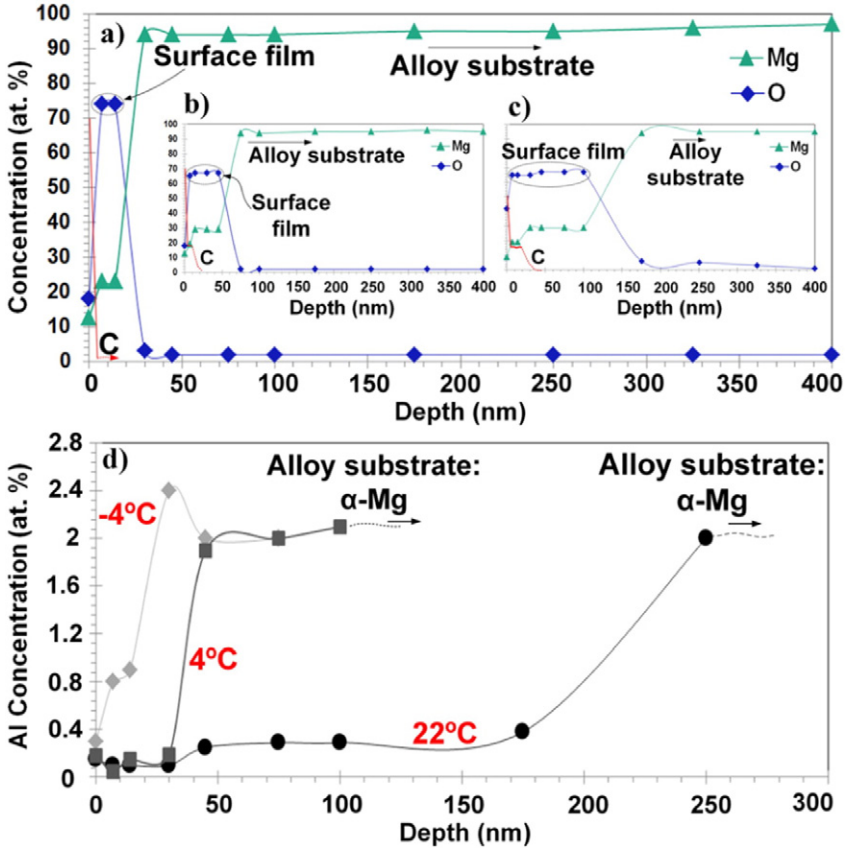

Fig. 3. AES depth profiles (area: 5 × 5 μm^2) from α-Mg grains in alloy AZ91D (CO_2: 400 ppm, time: 672 h); (a) O, C and Mg content at −4, (b) 4, (c) 22 °C, and (d) Al content in the film formed at the three temperatures.

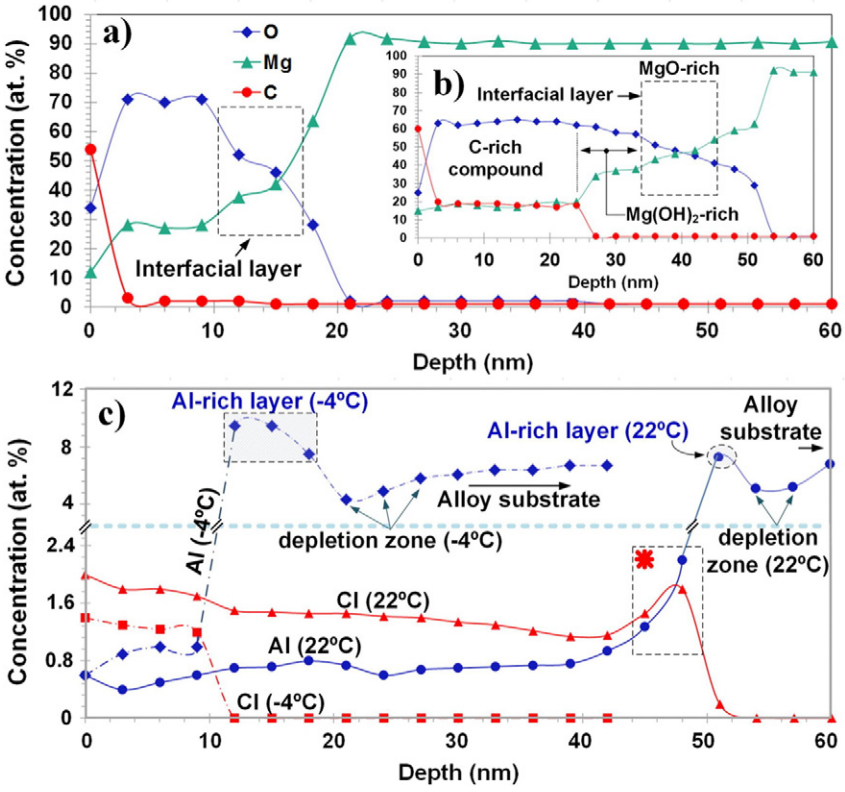

Fig. 4. AES depth profiles (area: 2 × 2 μm^2) from inter-dendritic regions in alloy AZ91D (CO_2: 400 ppm, NaCl: 10 μg/cm^2, time: 672 h); (a) at −4, (b) at 22 °C, and (c) Al and Cl content in the film formed at −4 (hatched lines) and 22 °C (full lines).

not exhibit a top carbonate-containing layer (Fig. 3a). Also, at −4 °C, the film exhibited an Al-enriched layer (~2.4 at.%) at the alloy/film interface, which was not evident at 4 and 22 °C (Fig. 3d).

Another set of exposures of alloy RC AZ91D were performed in the presence of a small amount of NaCl (10 μg/cm^2). In this case, the surface film formed on the inter-dendritic regions (containing ~7.5 ± 0.4 at.% Al) was examined. The strong temperature dependence of the corrosion rate of this alloy in the presence of NaCl was already mentioned (Fig. 1a and Fig. 2). Similar to the results in Fig. 3, the surface film formed at −4 °C was thinner (~15 nm) than at 22 °C (~53 nm) (Figs. 4a, b). While the overall film composition and the film layer sequence were similar to the salt-free experiments there was a clear indication of MgO at both temperatures in this case (compare Figs. 3a and c and Fig. 4). The difference may be due to the better depth resolution of the analyses.

At both temperatures, Al was enriched in the bottom part of the corrosion film (Fig. 4c). At −4 °C the alumina-enriched zone was ~9 nm thick with a maximum Al content of 9.5 at.%, while at 22 °C it was 3 nm and had a maximum Al content of ~8 at.%. An inspection of Fig. 4 clearly shows that the Al enrichment is associated with oxygen and occurs in the corrosion film (together with MgO). Hence, it can be concluded that the enriched aluminum component is oxidized (Al^{3+}). Indeed, in the alloy substrate immediately below the film there is a corresponding depletion of Al of similar magnitude. This implies that Al has oxidized preferentially and then incorporated into the bottom of the film. This is unexpected considering the higher oxygen affinity of Mg compared to Al [19]. Several authors have reported Al enrichments in the corrosion films formed on Mg–Al alloys [7,8,20–22]. Similar to this study, Danaie et al. [7] concluded that the enriched Al was in the oxidized state. However, Cano et al. [23] argued that the enriched Al formed on AM30 was in the metallic state. According to Birbilis et al. [24], incongruent dissolution results in a surface enrichment of impurity elements in Mg. However, incongruent dissolution of an Mg–Al alloy would result in an accumulation of the nobler element (Al) in the metallic state rather than in the oxidized state, as observed in the present case. It has been argued that Al-rich layers present at the film/alloy interface contributes to the corrosion protection of Mg–Al alloys [20]. Indeed, the fact that alumina is much less soluble than MgO and $Mg(OH)_2$ at near neutral pH implies that the Al-enriched layer at the bottom of the film may enhance corrosion properties, especially regarding the anodic dissolution. Hence, it is suggested that the positive effect of alloy Al content on corrosion properties is due to the protective properties of the Al-enriched layer.

Chloride was detected in the film at both temperatures, the chloride concentration being significantly higher at 22 °C than at −4 °C (Fig. 4c). There are reports of Cl in films formed on Mg alloys, see *e.g.*, [7]. The accumulation of chloride in the Al^{3+}-enriched zone at the bottom of the film (Fig. 4c) implies that chloride has penetrated the $Mg(OH)_2$/MgO film. It is argued that the Cl enrichment at the film/alloy interface at 22 °C (see the region marked with a star in Fig. 4c) is an indication of an ongoing chloride-assisted breakdown of the Al-enriched part of the film. Pitting corrosion of Al in the presence of chloride has been extensively studied and it is generally accepted that the chloride ion plays a crucial part in the breakdown of the alumina passive film [25,26]. It is well established that chloride readily adsorbs on the film surface. Also, it is reported that Cl^- is incorporated in the alumina film and migrates towards the film/metal interface. Thus, the penetration of the alumina film by chloride appears to be an important part of the mechanism of Al pit initiation [27]. The process of inclusion and migration of chloride in the alumina film must involve the breaking of bonds within the film and is hence predicted to be thermally activated. It is argued that similar processes occur in the Al^{3+}-enriched zone at the bottom of the film formed on alloy AZ91D (compare Fig. 4). Thus, the temperature dependence of the corrosion rate of alloy AZ91D is attributed to the thermally activated chloride-assisted breakdown of the protective alumina component in the film.

In accordance with [12,13], results illustrated the better corrosion resistance of RC AZ91D than that of HPDC AZ91D. Interestingly, Fig. 1a showed that the effect of temperature on the rate of corrosion is greater for the RC alloys. Considering that the reported average Al content in the central parts of the α-Mg grains was 2.6 ± 0.1 wt.% in the HPDC AZ91D, while the corresponding value for the same alloy in the RC state was 3.9 ± 0.22 wt.% (see [13]), it is proposed that the tendency for the temperature dependence of Mg–Al alloy corrosion to be stronger in the RC state than in the HPDC state (Fig. 2) is partially linked to the higher Al content of the α-Mg grains in the former material.

The AES analysis in Fig. 4c shows that except for the film/alloy interface, the Al content in the film is rather low, on the order of 0.8 at.%, corresponding to a Mg/Al ratio of about 25, implying that the bulk of the film is Al depleted relative to the substrate. Notably, AES investigations of the films formed on several alloys exposed at 22 °C in the presence of NaCl showed that while the films formed on α-Mg were consistently thicker than in the inter-dendritic areas, the thickness of carbonate-containing layers was about the same. Hence, the carbonate layer made up a much larger fraction of the films in the inter-dendritic area, signifying that the carbonate layer thickness is correlated to the Al content in the substrate and in the film. AES investigations confirmed this relationship between substrate Al content and carbonate film thickness on two other samples exposed in the presence of NaCl (not shown). It is suggested that this dependence may be related to the formation of layered double hydroxides (LDHs). This class of compounds has a structure related to brucite with the formula $[M^{+2}_{1-x}M^{+3}_x(OH)_2]^{+x}A^{-n}_{x/n} \times mH_2O$, where M^{+2} is a divalent metal (*e.g.* Mg^{2+}), M^{+3} a trivalent metal (*e.g.*, Al^{3+}) and A^{-n}, an anion [28]. Substituting Mg^{2+} in brucite by a trivalent ion, such as $A1^{3+}$ causes an excess positive charge which is compensated for by introducing anions in the interlayer region between the two hydroxide sheets. These anions can be hydroxide as in the case of meixnerite ($Mg_6Al_2(OH)_{12}4H_2O$), which was reported to form a corrosion product on Mg–Al alloys under CO_2-free conditions [3]. In the presence of CO_2, hydroxide in the charge-compensating layer reacts to form carbonate, often in non-crystalline form [28]. The LDHs are efficient CO_2 absorbers [28] and have been reported in some cases to protect against corrosion [29,30]. Whether LDHs are important in Mg–Al alloy corrosion remains an open question that will be addressed by us in a future study.

In summary, it was found that Al influences corrosion of Mg alloys in the following ways; (*a*) an increase in the Al content decreases the rate of corrosion, (*b*) Al content is responsible for the positive correlation between corrosion rate and temperature, the magnitude of the temperature effect being proportional to Al content, and (*c*) the influence of the cast microstructure on corrosion is partly related to the Al concentration in the α-Mg grains. In atmospheric corrosion, these effects of Al are associated to an Al^{3+}-enriched layer, which is formed in the bottom of the thin surface film. A corresponding Al depletion zone was detected in the alloy immediately below the film. It was discussed that the temperature effect is directly linked to a chloride-assisted breakdown of the Al^{3+}—rich in the bottom part of the film. It was also noted that the thickness of the surface carbonate layer increased with an increase in the Al content of the substrate. This effect was suggested to depend on the formation of LDHs.

Acknowledgments

The authors would like to deeply thank the Swedish Foundation for Strategic Research (SSF) (Grant number: RMA08-0138) for funding this research.

References

[1] S. Thomas, N.V. Medhekar, G.S. Frankel, N. Birbilis, Curr. Opin. Solid State Mater. Sci. 19 (2015) 85–94.
[2] N. Birbilis, A.D. King, S. Thomas, G.S. Frankel, J.R. Scully, Electrochim. Acta 132 (2014) 277–283.

[3] A. Atrens, G.-L. Song, M. Liu, Z. Shi, F. Cao, M.S. Dargusch, Adv. Eng. Mater. 17 (2015) 400–453.
[4] M. Esmaily, D.B. Blücher, R.W. Lindstrom, J.E. Svensson, L.G. Johansson, J. Electrochem. Soc. 162 (2015) C260–C269.
[5] M. Shahabi-Navid, M. Esmaily, J.E. Svensson, M. Halvarsson, L. Nyborg, Y. Cao, L.G. Johansson, J. Electrochem. Soc. 61 (2014) C277–C287.
[6] Z. Pu, S. Yang, G.-L. Song, O.W. Dillon Jr., D.A. Puleo, I.S. Jawahir, Scr. Mater. 65 (2011) 520–523.
[7] M. Danaie, R.M. Asmussen, P. Jakupi, D.W. Shoesmith, G.A. Bottona, Corros. Sci. 77 (2013) 151–163.
[8] R.M. Asmussen, P. Jakupi, M. Danaie, G.A. Bottonb, D.W. Shoesmith, Corros. Sci. 75 (2013) 114–122.
[9] H. Ha, H. Kim, S. Baek, B. Kim, S. Sohn, H. Shin, H.Y. Jeong, S.H. Park, C.D. Yim, B.S. You, J.G. Lee, S.S. Park, Scr. Mater. 109 (2015) 38–43.
[10] R.K. Singh Raman, N. Birbilis, J. Efthimiadis, Corros. Eng. Sci. Technol. 39 (2004) 346–350.
[11] M. Esmaily, N. Mortazavi, M. Shahabi-Navid, J.E. Svensson, M. Halvarsson, L. Nyborg, M. Wessén, A.E.W. Jarfors, L.G. Johansson, J. Electrochem. Soc. 162 (2015) C85–C95.
[12] M. Esmaily, N. Mortazavi, J.E. Svensson, M. Halvarsson, D.B. Blücher, A.E.W. Jarfors, M. Wessén, L.G. Johansson, J. Electrochem. Soc. 162 (2015) C311–C321.
[13] M. Esmaily, M. Shahabi-Navid, J.E. Svensson, M. Halvarsson, L. Nyborg, Y. Cao, L.G. Johansson, Corros. Sci. 90 (2015) 420–433.
[14] J.D. Hanawalt, C.E. Nelson, J.A. Peloubet, Trans. Metall. Soc. AIME 147 (1942) 273–299.
[15] G. Song, A. Atrens, Adv. Eng. Mater. 1 (1999) 1–33.
[16] M. Liu, P.J. Uggowitzer, A.V. Nagasekhar, P. Schmutz, M. Easton, G.L. Song, A. Atrens, Corros. Sci. 51 (2009) 602–619.
[17] J.H. Nordlien, S. Ono, N. Masuko, K. Nisancioglu, J. Electrochem. Soc. 142 (1995) 3320–3322.
[18] M.P. Brady, G. Rother, L.M. Anovitz, K.C. Littrell, K.A. Unocic, H.H. Elsentriecy, G.L. Song, J.K. Thomson, N.C. Gallego, B. Davis, J. Electrochem. Soc. 162 (2015) C140–C149.
[19] I. Barin, Thermochemical Data of Pure Substances, third ed. VCH Verlagsgesellschaft mbH, 2008.
[20] J.H. Nordlien, K. Nisancioglu, S. Ono, N. Masuko, J. Electrochem. Soc. 14 (1997) 461–466.
[21] K.A. Unocic, H.H. Elsentriecy, M.P. Brady, H.M. Meyer III, G.L. Song, M. Fayek, R.A. Meisner, B. Davis, J. Electrochem. Soc. 161 (2014) C302–C311.
[22] R.C. Phillips, J.R. Kish, Corrosion 69 (2013) 813–820.
[23] P. Cano, J.R. McDermid, J.R. Kish, J. Electrochem. Soc. 162 (2015) C732–C740.
[24] N. Birbilis, T. Cain, J.S. Laird, X. Xia, J.R. Scully, A.E. Hughes, ECS Electrochem. Lett. 4 (2015) C34–C37.
[25] P.M. Natishan, W.E. O'Grady, J. Electrochem. Soc. 161 (2014) C421–C432.
[26] H.H. Strehblow, Mechanisms of Pitting Corrosion in Corrosion Mechanisms in Theory and Practice, Basel, Marcel Dekker, New York, 2002.
[27] G.S. Frankel, J. Electrochem. Soc. 145 (1998) 2186–2198.
[28] X. Duan, D.G. Evans, Layered Double Hydroxides, Structure and Bonding, Springer-Verlag, Berlin, Heidelberg, 2006.
[29] R.B. Leggat, W. Zhang, R.G. Buchheit, S.R. Taylor, Corrosion 58 (2002) 322–328.
[30] R.G. Buchheit, J. Appl. Electrochem. 28 (1998) 503–510.